

Supplemental Information

Graphene plasmonics for ultrasensitive imaging-based molecular fingerprints detection

Chengdong Tao,^a Chuanbao Liu,^{b,*} Yongliang Li,^a Lijie Qiao,^a Ji Zhou,^c and Yang Bai^{a,†}

^a Beijing Advanced Innovation Center for Materials Genome Engineering, Institute for Advanced Materials and Technology, University of Science and Technology Beijing, Beijing 100083, China.

^b School of Materials and Engineering, University of Science and Technology Beijing, Beijing 100083, China.

^c State Key Laboratory of New Ceramics and Fine Processing, School of Materials Science and Engineering, Tsinghua University, Beijing 100084, China.

Corresponding authors: *cbliu@ustb.edu.cn; †baiy@mater.ustb.edu.cn

Supplemental Note 1. The surface conductivity of graphene.

The surface conductivity σ_s of graphene includes the contribution of both intraband and interband electronic transitions:

$$\begin{aligned}\sigma_s(\omega) &= \sigma_s^{\text{intra}}(\omega) + \sigma_s^{\text{inter}}(\omega) \\ \sigma_s^{\text{intra}}(\omega) &= \frac{2ie^2k_B T}{\pi\hbar^2(\omega + i\tau^{-1})} \ln \left[2 \cosh \left(\frac{E_F}{2k_B T} \right) \right] \\ \sigma_s^{\text{inter}}(\omega) &= \frac{e^2}{4\hbar} \left[\frac{1}{2} + \frac{1}{\pi} \arctan \left(\frac{\hbar\omega - E_F}{2k_B T} \right) - \frac{i}{2\pi} \ln \frac{(\hbar\omega + E_F)^2}{(\hbar\omega - E_F)^2 + (2k_B T)^2} \right]\end{aligned}\quad (1)$$

in which k_B is the Boltzmann's constant, \hbar is the reduced Planck's constant, ω is the angular frequency, τ is the relaxation time, and E_F is the Fermi level of graphene.

Supplemental Note 2. The effective permittivity of A/G-IgG protein bilayer.

The effective permittivity of A/G-IgG protein bilayer is described as a function of filling factor f according to the Maxwell-Garnet equivalent medium theory,

$$\varepsilon_{eff} = f \cdot \varepsilon_p + (1 - f) \quad (2)$$

Here, ε_p is the relative permittivity of A/G-IgG protein bilayer. The effective permittivities of protein bilayer with different filling factors are shown in Figure S2.

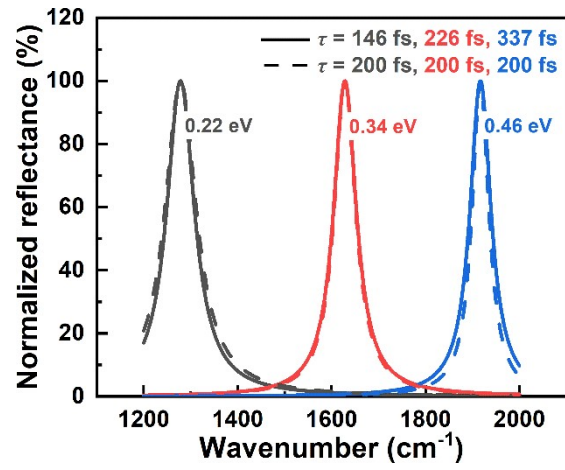


Fig. S1. Under different Fermi levels, the normalized reflectance spectra at varying relaxation times and constant relaxation time 200 fs, respectively.

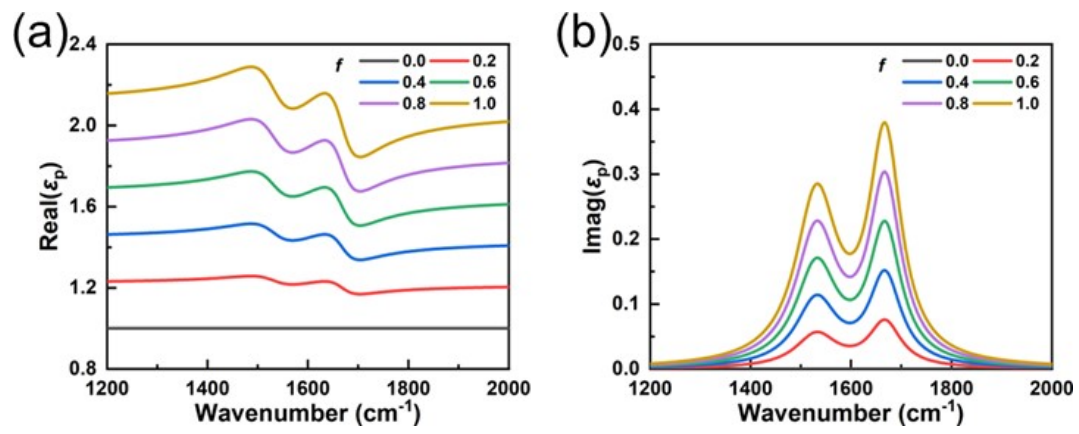


Fig. S2. The effective permittivity ϵ_p of A/G-IgG protein bilayer. (a) The real part of ϵ_p . (b) The imaginary part of ϵ_p .

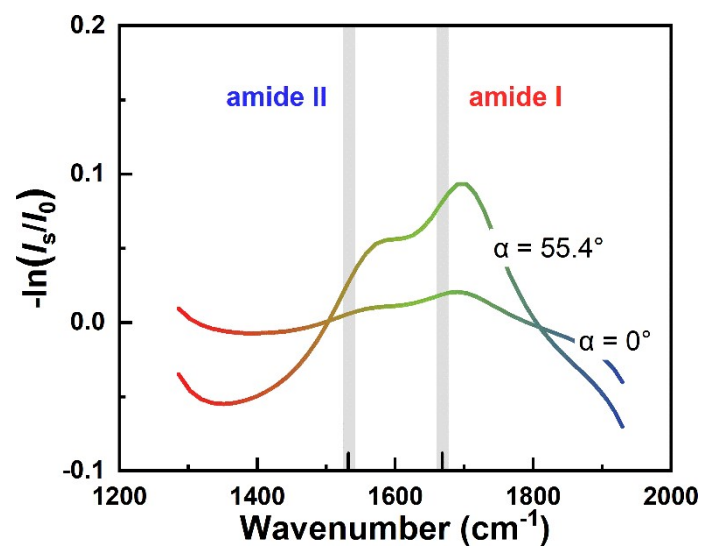


Fig. S3. The absorption signals calculated from light intensity spectra $-\ln(I_s/I_0)$ with incident angle $\alpha = 0^\circ$ and $\alpha = 55.4^\circ$.

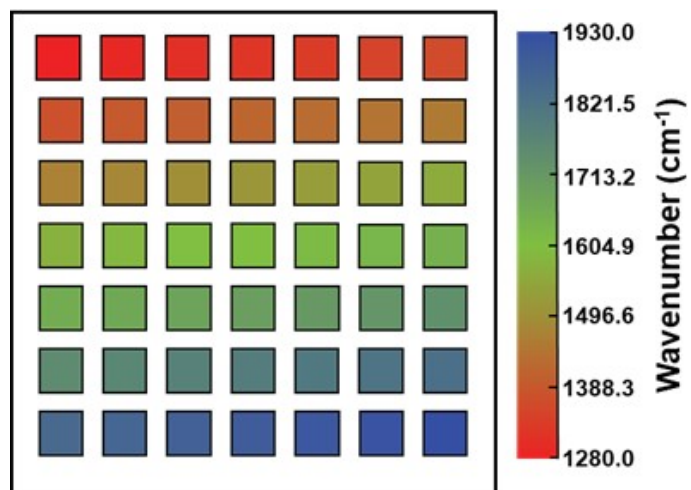


Fig. S4. Wavenumbers of each color block for imaging-based fingerprints detection of A/G-IgG protein bilayer.

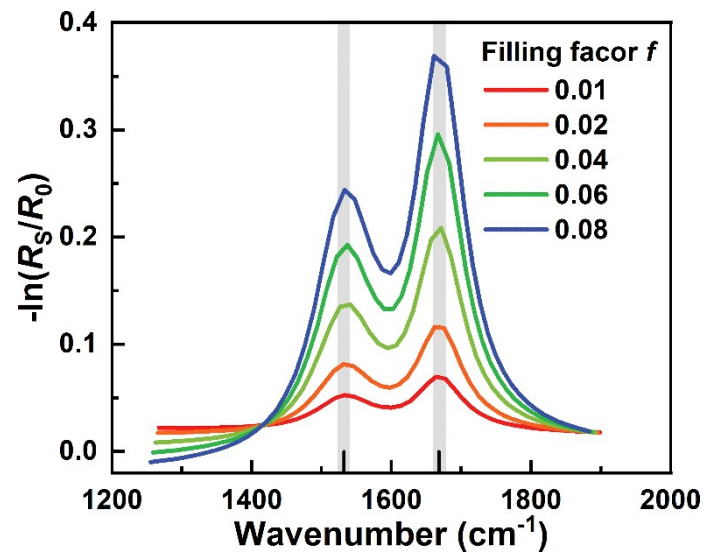


Fig. S5. The absorption bands of different amounts of protein physisorption revealed by the absorbance signals calculated from reflectance spectra $-\ln(R_s/R_0)$.

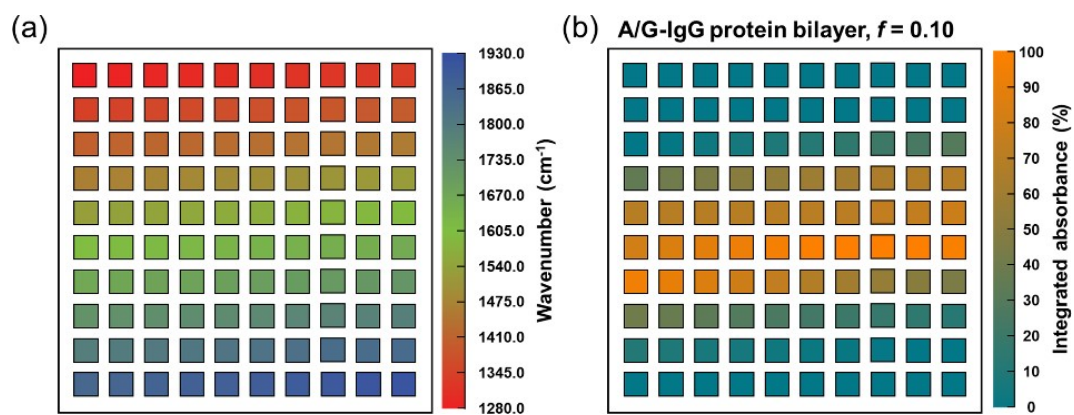


Fig. S6. The improved wavenumber's resolution in imaging-based fingerprints detection of A/G-IgG protein bilayer. (a) Wavenumbers of each color block for imaging-based fingerprints detection of A/G-IgG protein bilayer. (b) Schematic of integrated absorbance map after 10% protein bilayer physisorption.

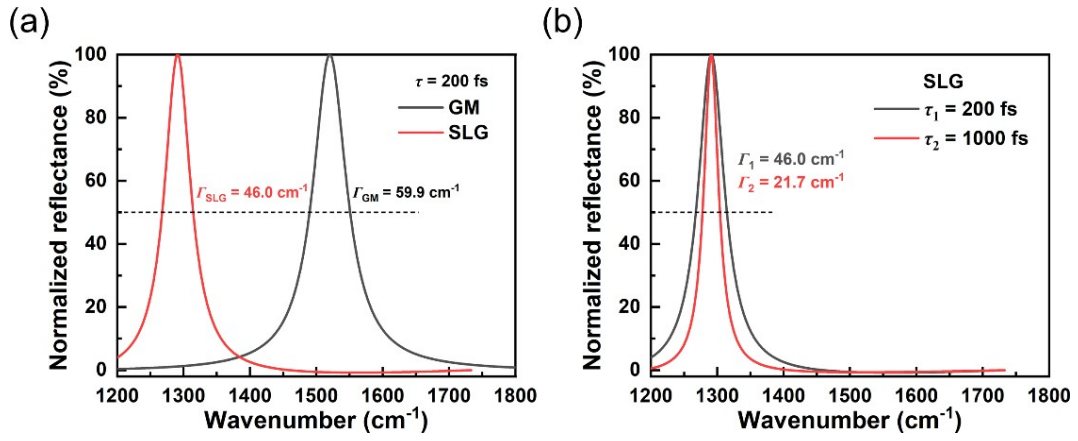


Fig. S7. The normalized reflectance spectra of the graphene metasurface and the graphene/silicon hybrid structure under the same relaxation time 200 fs. (b) The normalized reflectance spectra of the graphene/silicon hybrid structure at different relaxation times.

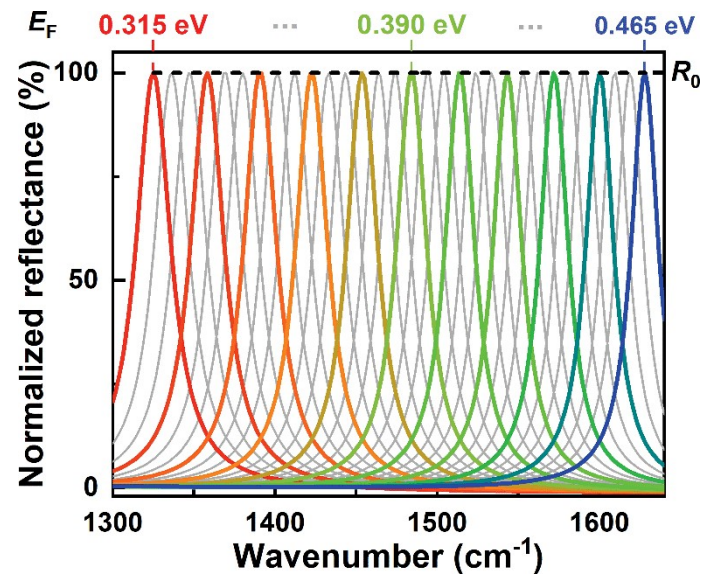


Fig. S8. Normalized reflectance spectra of the graphene/silicon grating hybrid structure with different Fermi levels.

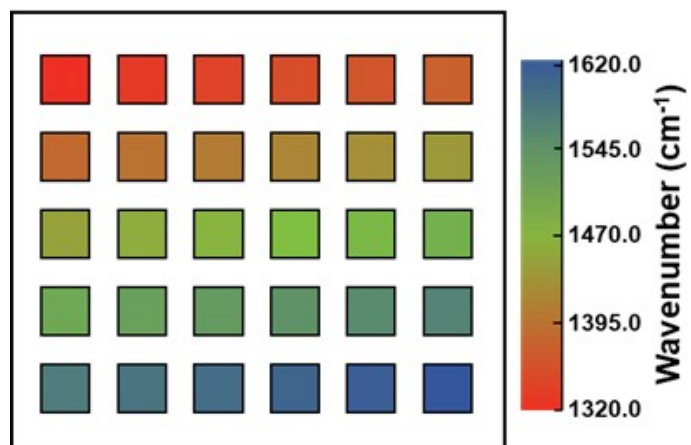


Fig. S9. Wavenumbers of each color block for imaging-based fingerprint detection of PE polymer layer.

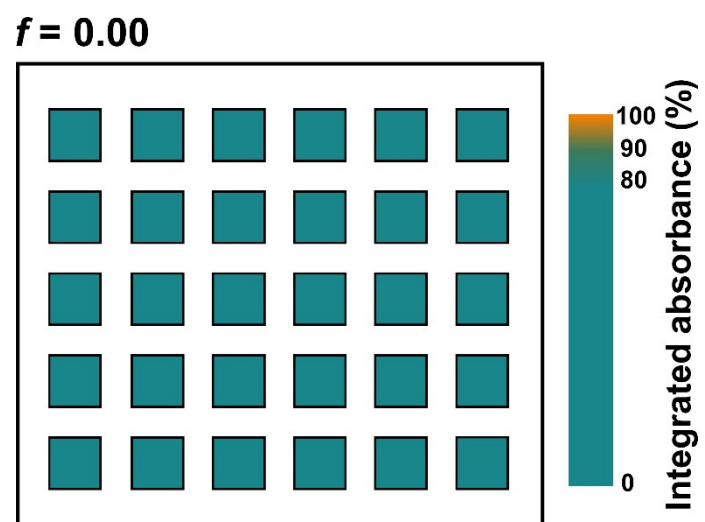


Fig. S10. Schematic of the integrated absorbance signal before PE molecule physisorption.

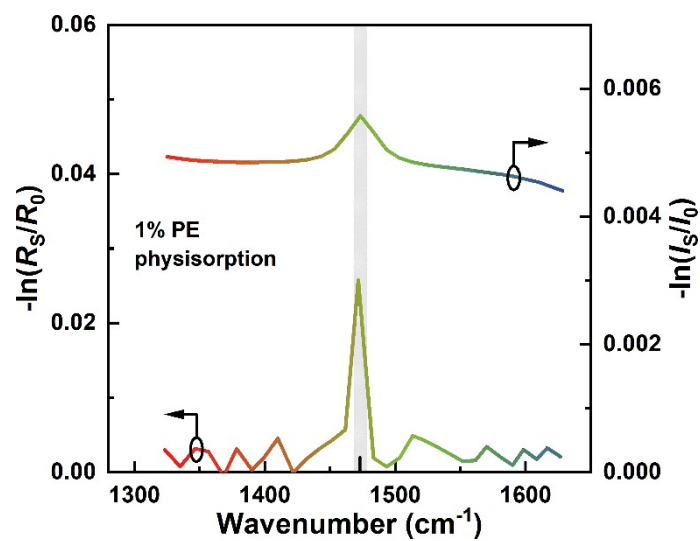


Fig. S11. The absorption signature of 1% PE layer physisorption revealed by absorbance signal calculated from reflectance spectra $-\ln(R_s/R_0)$ and absorbance signal calculated from light intensity spectra $-\ln(I_s/I_0)$, respectively.

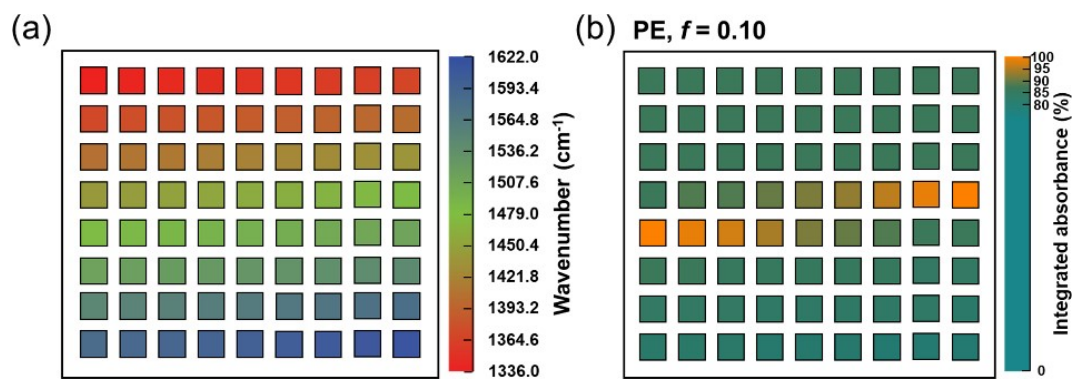


Fig. S12. The improved wavenumber's resolution in imaging-based fingerprint detection of PE. (a) Wavenumbers of each color block for imaging-based fingerprints detection of PE. (b) Schematic of integrated absorbance map after 10% PE physisorption.